IAEA Technical Committee Meeting on ECE and ECRH
7th Joint Workshop on ECE and ECRH (EC-7)
Hefei,Anhui (P. R. China) 8-11 May, 1989.

VELOCITY SPECTRA OF EMISSION AND ABSORPTION IN ELECTRON-CYCLOTRON RADIATION

I. Fidone, G. Giruzzi, G. Chiozzi[a], V. Krivenski[b]

ASSOCIATION EURATOM-CEA SUR LA FUSION
Département de Recherches sur la Fusion Contrôlée
Centre d'Etudes Nucléaires de Cadarache
13108 - Saint-Paul-lez-Durance (FRANCE)

[a] Dipartimento di Fisica, Università di Ferrara, Ferrara (ITALY)

[b] Asociacion EURATOM-CIEMAT para fusion, CIEMAT, Madrid, (Spain).

VELOCITY SPECTRA OF EMISSION AND ABSORPTION IN ELECTRON-CYCLOTRON RADIATION

I. Fidone, G. Giruzzi, G. Chiozzi[a], V. Krivenski[b]

ASSOCIATION EURATOM-CEA SUR LA FUSION
Département de Recherches sur la Fusion Contrôlée
Centre d'Etudes Nucléaires de Cadarache
13108 - Saint-Paul-lez-Durance (FRANCE)

[a] Dipartimento di Fisica, Università di Ferrara, Ferrara (ITALY)

[b] Asociacion EURATOM-CIEMAT para fusion, CIEMAT, Madrid, (Spain).

Abstract

Selective electron-cyclotron processes are investigated using the phase-space spectra of emission and absorption for arbitrary momentum distribution functions. It is shown that, in general, for a system of electrons a sharp resonant velocity does not exist because of the finite half-width of the radiation spectra. However, the maximum of power absorption (emission) determines the velocity range of the predominant electrons and can represent the counterpart of the one-particle relativistic resonance velocity. It is also shown that, in contrast with the Maxwellian distribution, for a non-thermal plasma the emission and absorption spectra are not proportional and therefore emission and absorption depend on electrons in different regions of the accessible phase space.

I. Introduction

Emission and absorption of electron-cyclotron waves in a plasma with a given momentum distribution are described by the emission and absorption coefficients and their determination is a central issue in cyclotron radiation processes and related applications as, for instance, current drive and diagnosis of non-thermal electrons. However, the emission and absorption coefficients are momentum integrated quantities and will not display any specific feature of selective wave emission and absorption which are of paramount interest for current drive and plasma probing. In order to investigate momentum selective resonance processes, it is necessary to analize the emission and absorption profiles in momentum space. The velocity spectra define the accessible region in the phase space where the resonant processes take place. In particular, the maxima of the emission and absorption spectra characterize the predominant contributions of the resonant electrons. As is known, the resonant interaction between an electron of given momentum and a wave is determined by the one-particle relativistic resonance relation. This is often used to determine the resonant velocity of a system of electrons. This qualitative estimate of the resonant velocity is in general incorrect. In fact, for a system of

electrons the counterpart of the one-particle resonant velocity is naturally given by the maximum of the emission and absorption spectra. In contrast with the one-particle resonant velocity, the location of the maximum in the parallel and perpendicular directions is well determined. However, the half-width of the radiation spectra is in general comparable with the value at the maximum and therefore, for a system of electrons, it is not possible to define a sharp resonant velocity.

The paper is devoted to this problem and it is organized as follows. In Sec. II, we present the general formulation of the theory of electron-cyclotron radiation. In Sec. III, we discuss several examples of momentum distributions of current interest, i.e., the isotropic Maxwellian, the loss-cone distribution and the lower-hybrid sustained fast tail; for each case a typical application is discussed. In the first case, we derive an analytical formula for the maximum of the absorption profile and discuss its relevance in the problem of electron-cyclotron current drive for arbitrary harmonics. The loss-cone distribution is used to illustrate the deviation between the predominant groups of electrons contributing to the processes of emission and absorption for a given wave. Finally, in the last case we discuss the resonant velocity for a fast tail and the relevance of the perpendicular momentum component on the parallel resonant velocity for a system of electrons, a central issue in the diagnosis of a current-carrying tail using electron-cyclotron wave emission and transmission. The conclusion is given in Sec. IV.

II. General theory of emission and absorption.

The global results of emission and absorption are the cumulative contributions of electrons in a given velocity range, thus,

$$\alpha(\omega) = \int d\vec{p}\ \alpha(\vec{p}) = \sum_{n=1}^{\infty} \int d\vec{p}\ \alpha_n(\vec{p}) \ , \qquad (1)$$

where $\vec{p}$ is the electron momentum. For cyclotron resonance processes $\alpha_n(p) \propto \delta(\gamma - Y_n - N_{\parallel} p_{\parallel}/mc)$, where $\gamma^2 = (1+p^2/m^2c^2)$, $Y_n = n\omega_c/\omega$, $N_{\parallel}$ is the parallel refractive index and m is the electron rest mass. Using the δ-function, we obtain the one-particle resonance relation

$$\gamma = Y_n + N_{\parallel} p_{\parallel}/mc \ ,$$

from which

$$(p_{\perp}/mc)^2 = (N_{\parallel} p_{\parallel}/mc + Y_n)^2 - 1 - (p_{\parallel}/mc)^2 = v_{\perp R}^2 \ .$$

Since $p_{\perp}^2 > 0$, we obtain $p_- < p_{\parallel} < p_+$, and

$$\alpha(\omega) = \sum_{n=1}^{\infty} \int_{p_-}^{p_+} dp_{\parallel}\ W_n(p_{\parallel}) \ ,$$

where

$$p_{\pm} = mc \left[N_{\parallel} Y_n \pm (N_{\parallel}^2 - 1 + Y_n^2)^{1/2} \right] / (1 - N_{\parallel}^2)$$

and we consider for simplicity the case of most interest, i.e., $|N_{\parallel}|<1$. $W_n(p_{\parallel})$ is proportional to the power absorption per unit interval in momentum space. Now, from Poynting theorem $\alpha(\omega)=W/S$, where W is the power absorption per unit volume and S is the magnitude of the Poynting vector, and

$$W = n_e \int d\vec{p}\, mc^2\gamma\, (\partial f/\partial t)_{cy} , \tag{2}$$

where n_e is the electron density,

$$(\frac{\partial f}{\partial t})_{cy} = 4\pi e^2 \sum_{n=1}^{\infty} \int_{-\infty}^{\infty} dN_{\parallel}\, (\gamma/p_{\perp}) L_n D_n \delta(\gamma - Y_n - N_{\parallel}p_{\parallel}/mc) L_n f , \tag{3}$$

$\gamma L_n = Y_n(\partial/\partial p_{\perp}) + (N_{\parallel}p_{\perp}/mc)(\partial/\partial p_{\parallel})$, $\quad D_n = (p_{\perp}/8\omega)|\vec{E}\cdot\vec{\Pi}_n|^2$,
$\vec{E}$ is the wave electric field, $\Pi_{1n}=nJ_n(\rho)/\rho$, $\Pi_{2n}=-iJ_n'(\rho)$, $\Pi_{3n}=(p_{\parallel}/p_{\perp})J_n(\rho)$, $\rho = k_{\perp}p_{\perp}/m\omega_c$, $-e$ is the electron charge, and $\vec{k}$ is the wave vector. Using Eqs. (2) and (3), we obtain

$$\alpha(\omega) = \sum_{n=1}^{\infty} \int_{v_-}^{v_+} dv_{\parallel}\, W_n(v_{\parallel}) ,$$

$$W_n(v_{\parallel}) = -2\pi(mc)^3\omega_p^2[\gamma(D_n/S)L_n f]_{v_{\perp}=v_{\perp R}} , \tag{4}$$

$\vec{v} = \vec{p}/mc$, $v_{\perp R}^2 = \gamma_n^2 - \gamma_{\parallel}^2$, $\gamma_n = Y_n + N_{\parallel}v_{\parallel}$, $\gamma_{\parallel} = (1+v_{\parallel}^2)^{1/2}$ and ω_p is the plasma frequency. The emission coefficient $\beta(\omega)$ is obtained from the absorption coefficient $\alpha(\omega)$ using the transformation[1]

$$L_n f \rightarrow -(\omega^2/8\pi^3c^2)p_{\perp}f/m\gamma ,$$

hence,

$$\beta(\omega) = \sum_{n=1}^{\infty} \int_{v_-}^{v_+} dv_{\parallel}\, G_n(v_{\parallel}) ,$$

where

$$G_n(v_{\parallel}) = (\omega^2/8\pi^3c^2)2\pi(mc)^3\omega_p^2 c[(D_n/S)v_{\perp}f]_{v_{\perp}=v_{\perp R}} . \tag{5}$$

Equations (4) and (5) determine the momentum spectra of the absorption and emission coefficients. W_n (G_n) describes the relative role of the electrons in a given velocity range on the global absorption (emission). In particular, the value of $v_{\parallel}$ for which W_n (G_n) is maximum characterizes the group of electrons which yields the predominant contribution to wave absorption (emission). In the case of a sharp maximum it is possible to define the resonant velocity for a system of electrons. Unfortunately, for most systems of practical interest this is not the case. Note that, for a Maxwellian distribution, $G_n(v_{\parallel}) = B_0 W_n(v_{\parallel})$, $B_0 = \omega^2 T_e/8\pi^3c^2$, and

we obtain that the electrons giving the predominant contribution to emission and absorption lie in the same range of velocities. For non-Maxwellian momentum distributions, $G_n(v_\parallel)$ is not in general proportional to $W_n(v_\parallel)$ and emission and absorption depend on electrons in different regions of the momentum space.

III. Applications

III.a Emission and absorption in a Maxwellian plasma.

We first consider a Maxwellian distribution. In this case

$$W_n(v_\parallel) = [\omega_p^2\mu^2/16\omega K_2(\mu)]v_{\perp R}^2\,[|\vec{E}\cdot\vec{\Pi}_n|^2/S]_{v_\perp=v_{\perp R}} \exp(-\mu\gamma_n) \quad , \qquad (6)$$

where $\mu = mc^2/T_e$. As discussed in Ref. 2, for $N_\parallel \neq 0$, $W_n(v_\parallel)$ is maximum at $v_\parallel = v_{\parallel n}$ given by ($N_\parallel > 0$)

$$v_{\parallel n} = [N_\parallel Y_n - (N_\parallel^2 - 1 + Y_n^2 - Y_n^2\Psi)^{1/2}]/(1-N_\parallel^2) \quad , \quad v_{\perp n}^2 = Y_n^2\Psi/(1-N_\parallel^2) \quad ,$$

$$\Psi = \frac{1 + (N_\parallel^2 - 1 + Y_n^2)/Y_n^2 - [(1-N_\parallel^2)^2/Y_n^4 + 4\lambda(N_\parallel^2 - 1 + Y_n^2)/Y_n^2]^{1/2}}{2(1-\lambda)} \quad ,$$

$\lambda = (N_\parallel \mu Y_n)^2/4n^2(1-N_\parallel^2)^2$. For small n we have

$v_{\perp n}^2 \simeq (2n/N_\parallel\mu)(N_\parallel^2 - 1 + Y_n^2)^{1/2}$, $\quad \mathrm{sgn}(v_{\parallel n}) = \mathrm{sgn}(1 - Y_n^2 + 2nY_n/\mu)$.

For $Y_n < 1$ and $N_\parallel > 0$ we obtain $v_{\parallel n} > 0$. For $Y_n > 1$ and $N_\parallel > 0$, we obtain $v_{\parallel n} < 0$ except for

$$Y_n < n/\mu + (1 + n^2/\mu^2)^{1/2} \simeq 1 + n/\mu \quad .$$

We obtain that for the predominant group of electrons $v_\parallel$ changes sign if Y_n crosses the value $Y_n = 1$. This is illustrated by the two examples shown in Fig. 1 (ordinary mode, $N_\parallel = 0.42$, $\omega_c/\omega = 0.933$), and in Fig. 2 (extraordinary mode, $N_\parallel = 0.766$, $\omega_c/\omega = 1.2$), for $n = 1$ and $T_e = 3$ keV. The same conclusions hold for the emission, since for a Maxwellian distribution $W_n(v_\parallel)$ is proportional to $G_n(v_\parallel)$.

It is of interest to relate $W_n(v_\parallel)$ with the current drive efficiency. Using the impulse-response method, the incremental efficiency is given by[2,3]

$$\delta J_{cy}/\delta P_{cy} = (e/mc)[N_\parallel + v_\parallel\gamma\nu(\gamma)\frac{\partial}{\partial\gamma}(\frac{1}{\gamma\nu(\gamma)})][\gamma\nu(\gamma)]^{-1},$$

where

$$\delta P_{cy} = (4\pi e^2/m)\sum_{n=1}^{\infty} D_n\delta(\gamma - n\omega_c/\omega - N_\parallel v_\parallel)L_n f \quad .$$

Combining the two equations we obtain

$$J_{cy}/P_{cy} = \sum_{n=1}^{\infty} \int_{v_-}^{v_+} dv_{\parallel} g(v_{\parallel})\, W_n(v_{\parallel}) \Big/ \sum_{n=1}^{\infty} \int_{v_-}^{v_+} dv_{\parallel}\, W_n(v_{\parallel}) \quad , \tag{7}$$

where

$$g(v_{\parallel}) = (e/mc)[N_{\parallel} + v_{\parallel}\Gamma(\gamma_n)]/\gamma_n \nu(\gamma_n) \ ,$$

and for the ion charge Z=1

$$\nu(\gamma) = (4\pi e^4 n_e \Lambda/m^2c^3)(\gamma-1)^{3/2} \ / \ (\gamma+1)^{1/2}(\gamma^2 - 2\gamma \ln\gamma - 1) \ ,$$

$$\Gamma(\gamma) = [2\gamma^2(\gamma+2)\ln\gamma - (4\gamma-1)(\gamma^2-1)][\gamma\,(\gamma^2-1)(\gamma^2 - 2\gamma \ln\gamma - 1)]^{-1} \ ,$$

where Λ is the Coulomb logarithm. It appears from Eq. (7) that in the low harmonics range of frequencies, $v_{\parallel_n}$ changes sign[4] for two adjacent harmonics and current cancellation due to harmonic overlap might occur. On the other hand, as shown in Ref. 2, for $n \gg 1$, $sgn(v_{\parallel_n}) = sgn(N_{\parallel})$ for any relevant value of Y_n and no cancellation occurs. This is illustrated in Fig. 3, where the resonant momenta are shown for $\omega/\omega_c \simeq 10.4$, $T_e = 50$ keV, $N_{\parallel} = 0.77$, poloidal angle $\chi = \pi/2$, and the relevant values of the harmonic number n. The trapping cone is also shown for $\varepsilon = r/R = 0.1$ (solid line) and 0.2 (dashed line).

III.b Emission and absorption by a loss-cone distribution.

In order to illustrate the deviation between $G_n(v_{\parallel})$ and $W_n(v_{\parallel})$, we consider the loss-cone momentum distribution

$$f = \frac{\mu_{\parallel}^{1/2}\mu_{\perp}^{1+\ell/2}}{(2\pi)^{3/2}(mc)^3} \frac{1}{2^{\ell/2}\Gamma(1+\ell/2)} v_{\perp}^{\ell} \exp(-\mu_{\perp}v_{\perp}^2/2 - \mu_{\parallel}v_{\parallel}^2/2)$$

where $\mu_{\perp} = mc^2/T_{\perp}$, $\mu_{\parallel} = mc^2/T_{\parallel}$ and ℓ is a given number representing the mirror effect. For simplicity, we consider a tenuous plasma, for which $N_{\perp}^2 = 1 - N_{\parallel}^2$. According to Eqs. (4-5), this implies that W_n and G_n vanish for $N_{\parallel} \to 1$. For $\ell = 0$ and $T_{\parallel} = T_{\perp}$, we obtain the Maxwellian distribution. For $\ell = 0$ but $T_{\parallel} \neq T_{\perp}$ Eqs. (4-5) yield

$$G_n/\bar{W}_n = \mu_{\perp}[\ Y_n\mu_{\perp} + N_{\parallel}\mu_{\parallel}v_{\parallel} \ ]^{-1} \ . \tag{8}$$

where $\bar{W}_n = W_n(v_{\parallel})B_0(\omega,T_{\perp})$. Since $G_n/\bar{W}_n$ is not constant in momentum space, Kirchhoff's law is not valid for the anisotropic Maxwellian distribution, as appears in Fig. 4, for n=2, $\omega = 2\omega_c$, $N_{\parallel} = 0.5$, $T_{\perp} = 50$ keV, and $T_{\parallel} = 2$ keV. However, Fig. 4 shows that the two processes are determined by electrons in the same ranges of $v_{\parallel}$ and $v_{\perp}$.

For a loss-cone distribution, i.e., $\ell \neq 0$, Eqs. (4-5) yield

$$G_n/\bar{W}_n = \mu_{\perp}[\ Y_n(\mu_{\perp} - \ell/v_{\perp R}^2) + N_{\parallel}\mu_{\parallel}v_{\parallel} \ ]^{-1} \ . \tag{9}$$

This equation shows that now the sign of $G_n/\bar{W}_n$ can change. In particular, for small $v_{\perp R}$, W_n can become negative, i.e., stimulated emission is dominant compared to "true" absorption. This is illustrated in Fig. 5,

for the parameters of Fig. 4 and ℓ=2. It appears that for the loss-cone distribution two distinct groups of electrons are mainly responsible for stimulated emission and "true" absorption, for $v_{\parallel} < 0.1$ and $v_{\parallel} > 0.1$, respectively. Note that, for $v_{\parallel} \simeq 0.1$, the spontaneous emission is maximum whereas the global absorption is practically zero. This illustrates the microscopic behaviour of a system of electrons for which the Kirchhoff's law is not applicable.

III.c Emission and absorption by the lower-hybrid tail.

We now discuss electron-cyclotron emission and absorption by a special non-Maxwellian system, i.e., the current carrying electron tail generated by lower-hybrid waves. In this case, the momentum distribution is computed by means of a 3-D Fokker-Planck code, solving the equation

$$\frac{\partial f}{\partial t} = \left\langle \left(\frac{\partial f}{\partial t}\right)_{LH} \right\rangle + \left\langle \left(\frac{\partial f}{\partial t}\right)_{coll} \right\rangle , \qquad (10)$$

where

$$\left(\frac{\partial f}{\partial t}\right)_{LH} = \frac{\partial}{\partial u_{\parallel}} D_{LH} \frac{\partial f}{\partial u_{\parallel}} ,$$

$(\partial f/\partial t)_{coll}$ is the high-velocity limit of the relativistic Fokker-Planck collision operator, the brackets < > denote flux-surface averaging in toroidal geometry and $u_{\parallel} = p_{\parallel}/p_e = p_{\parallel}/(mT_e)^{\frac{1}{2}}$. For the lower-hybrid diffusion coefficient we adopt a very simple model, i.e., we assume D_{LH} constant for $p_1 < p_{\parallel} < p_2$ and vanishing outside this interval. The values of p_1 and p_2 are related to the boundaries of the lower-hybrid $N_{\parallel}$ spectrum. In the following example we refer to typical Tore Supra parameters, i.e., a = 70 cm, R = 225 cm, T_e = 3 keV, $n_e = 5 \times 10^{13}$ cm^{-3}, and we choose $D_{LH} = 0.8$, $u_1 = p_1/p_e(0) = 3.8$, $u_2 = 7$. Equation (10) is solved for $0 \leq r \leq 40$ cm on eleven magnetic surfaces, until steady-state is attained. In Figs. 6 and 7 we present the parallel distribution $f_{\parallel}$ and the perpendicular temperature $T_{\perp}$ versus $u_{\parallel}$ for several values of r, i.e., a) r = 0, b) r = 20 cm, c) r = 40 cm. Note that the complicate spatial dependence of $f_{\parallel}$ and $T_{\perp}$ could hardly be described by simple models and its evaluation requires the use of a 3-D Fokker-Planck code. The distribution function shown in Figs. 6 and 7 is used to evaluate the absorption of electron-cyclotron waves. By an appropriate launching of the extraordinary mode it is possible to transfer electron-cyclotron wave energy to any desired region in ordinary and momentum spaces[5]. For instance, for B(0) = 4.5 Tesla, wave frequency f = 100 GHz, top launching at an angle φ = 105° with respect to the toroidal magnetic field, the maximum power deposition occurs at r = 16 cm, where ω_c/ω = 1.35. The location of maximum power deposition in momentum space is found by plotting $W_1(u_{\parallel})$ for the numerically computed distribution function, as shown in Fig. 8. Note that $v_{\parallel R}$ is appreciably different from v_+, where $W_1 = 0$. The value $v_{\parallel} = v_+$ is often considered as representative of the resonant velocity for the lower-hybrid sustained tail. Now, for $v_{\parallel} = v_+$ we obtain $v_{\perp} = 0$. The result of Fig. 8 clearly shows that for a system of electrons the finite value of $v_{\perp}$ is essential for determining both the $v_{\parallel}$ position of maximum absorption and the half-width of the absorption spectrum. It appears that most of the wave

power is absorbed for $7 < u_{\parallel} < 8$, i.e., in the far end of the electron tail. In this case, the position of the maximum of W_1 does not change during the quasilinear evolution of the electron distribution function at high electron cyclotron power, as also shown in Fig. 8 for $P_{EC} = 0.4$ MW. The localization in momentum space of the perturbation induced by the electron-cyclotron wave pulse at 100 GHz gives rise to a localized change in the absorption and emission coefficients of any electron-cyclotron wave used to probe the plasma. For instance, we now consider wave transmission and emission in the vertical direction, i.e., normal to the toroidal magnetic field and to its gradient, at frequencies close to the second harmonic, for the extraordinary mode. The transmission coefficient for an extraordinary wave propagating along a poloidal diameter is defined by

$$t_{rx}(\omega) = \exp[-\int_{-a}^{+a} dx\ \alpha_x(x)] \ ,$$

where x is the abscissa along the diameter. The radiative temperature T_{rx} of the radiation emerging at one of the two ends of the poloidal diameter $\pm a$, in the absence of wall reflections is defined by

$$T_{rx}(\pm a,\omega) = \frac{(2\pi)^3 c^2}{\omega^2} \int_{-a}^{+a} dx\ \beta_x(x) \exp[\ \mp \int_{x}^{\pm a} dx' \alpha_x(x')] \ ,$$

where α_x (β_x) is the absorption (emission) coefficient[6] for the extraordinary mode at the second harmonic. In Figs. 9 and 10, we show the incremental transmission coefficient and radiative temperature, respectively, i.e., the difference between those quantities in the presence and in the absence of the electron-cyclotron power. It appears that both the incremental spectra have pronounced peaks in frequency, related to the peak of $W_1(u_{\parallel})$. Transmission and emission measurements at the second harmonic can then help for an experimental investigation of selective resonance absorption near the fundamental gyrofrequency.

IV. Conclusions

The general problem discussed in this paper is the definition of the electron-cyclotron resonance velocity for a system of electrons with an arbitrary momentum distribution. This is a central problem in the theory of selective resonance processes as, for instance, current drive, electron heating via superthermal electrons , and diagnosis of non-Maxwellian distributions. The adopted procedure is naturally the study of the emission and absorption profiles in the momentum space. For electron momentum distributions for which the power absorption (emission) profile has a sharp maximum within the accessible phase space, the position of the maximum represents the counterpart of the one-particle resonance velocity. However, for the three cases of momentum distributions considered in the paper, i.e., the isotropic Maxwellian, the loss-cone, and the lower-hybrid sustained tail, we have found a relatively broad maximum determined by the perpendicualr temperature. Therefore, in general, it is only possible to determine the velocity

range of the electrons which give the predominant contribution to emission and absorption. The case of the resonant velocity for electron-cyclotron wave absorption by the fast lower-hybrid tail is particularly instructive. We have found that the maximum of power deposition differs appreciably from the value v_+ which is the solution of the simplified one-particle resonance (i.e., for $p_\perp = 0$). This is of relevance in the problem of radial control of the lower-hybrid current by electron-cyclotron wave absorption[5] and diagnosis of the tail distribution by electron-cyclotron wave transmission (emission) measurements[6]. This study has also shown the role of the appropriate Fokker-Planck code in the problem of diagnosing the superthermal electron distribution, since the absorption (emission) spectra are very sensitive to the perpendicular momentum distribution. We have also shown that for systems with inverted population distributions there is no simple relation between emitting and absorbing electrons resonating with a given wave. This is of relevance in the problem of radiation transfer. Finally, it is shown that the power absorption profile determines the efficiency of electron-cyclotron current drive and therefore an experimental investigation of the ratio J/P is in principle possible through wave transmission measurements of electron cyclotron waves.

References

1 BEKEFI, G. Radiation Processes in Plasmas (Wiley, New York, 1966), Chap.2.

2 FIDONE, I., GRANATA, G., JOHNER, J., Phys. Fluids **31** (1988) 2300.

3 FISCH, N.J., Rev. Modern Physics **59** (1987) 175.

4 SMITH, G.R., COHEN, R.H., MAU, T.K., Phys. Fluids **30** (1987) 3633.

5 FIDONE, I., GIRUZZI, G., KRIVENSKI, V., MAZZUCATO, E., ZIEBELL, L.F., Nucl. Fusion **27** (1987) 579.

6 FIDONE, I., GIRUZZI, G., GRANATA, G., MEYER, R.L., Phys. Fluids **26** (1983) 3284; GIRUZZI, G., FIDONE, I., GRANATA, G., MEYER, R.L., Phys. Fluids **27** (1984) 1704; KATO, K., HUTCHINSON, I.H., Phys. Fluids **30** (1987) 3809.

Figure captions

Fig. 1 $W_1(u_\parallel)$ for the ordinary mode, $\omega_c/\omega = 0.933$, $N_\parallel = 0.42$.

Fig. 2 $W_1(u_\parallel)$ for the extraordinary mode, $\omega_c/\omega = 1.2$, $N_\parallel = 0.766$.

Fig. 3 Trapping cones for $\chi = \pi/2$, $\varepsilon = 0.1$ (solid) and $\varepsilon = 0.2$ (dashed); locations of the resonant velocities $v_{\parallel n}$, $v_{\perp n}$, for $\omega/\omega_c = 10.4$, $T_e = 50$ keV, $N_\parallel = 0.77$, and $n = 7 - 14$.

Fig. 4 G_n and $\bar{W}_n$ in arbitrary units versus $v_\parallel$ for an anisotropic Maxwellian distribution and $n=2$, $\omega=2\omega_c$, $N_\parallel=0.5$, $T_\perp=50$ keV, $T_\parallel=2$ keV.

Fig. 5 As in Fig. 4 for a loss-cone distribution with $\ell=2$.

Fig. 6 $-\ln f_\parallel$ vs $u_\parallel\ \mathrm{sgn}(u_\parallel)$ for a) r=0; b) r=20 cm; c) r=40 cm.

Fig. 7 Perpendicular temperature in keV for the conditions of Fig. 6.

Fig. 8 $W_1(u_\parallel)$ for the distribution function shown in Figs. 6,7 and for $P_{EC} = 0.4$ MW.

Fig. 9 Incremental transmission Δt_{rx} vs frequency for $P_{EC} = 0.4$ MW.

Fig.10 Incremental emission ΔT_{rx} for the conditions of Fig. 9.

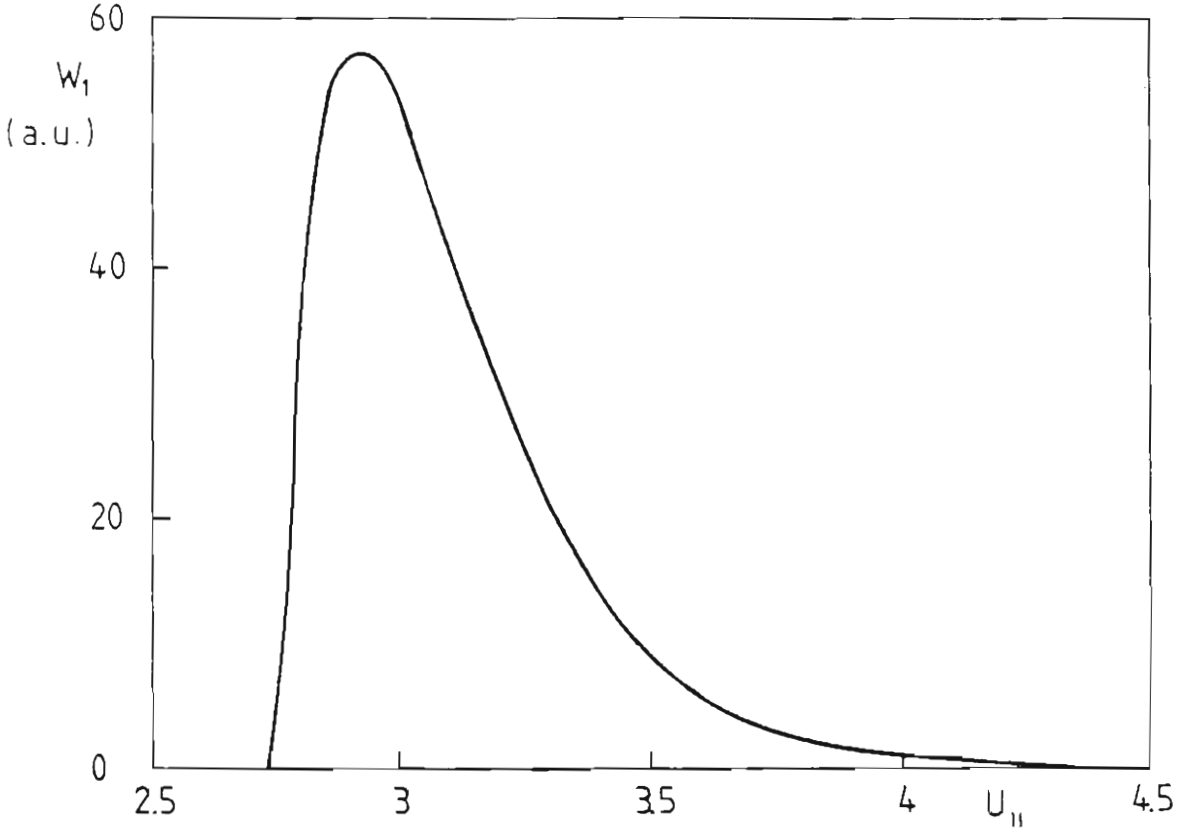

FIG.1

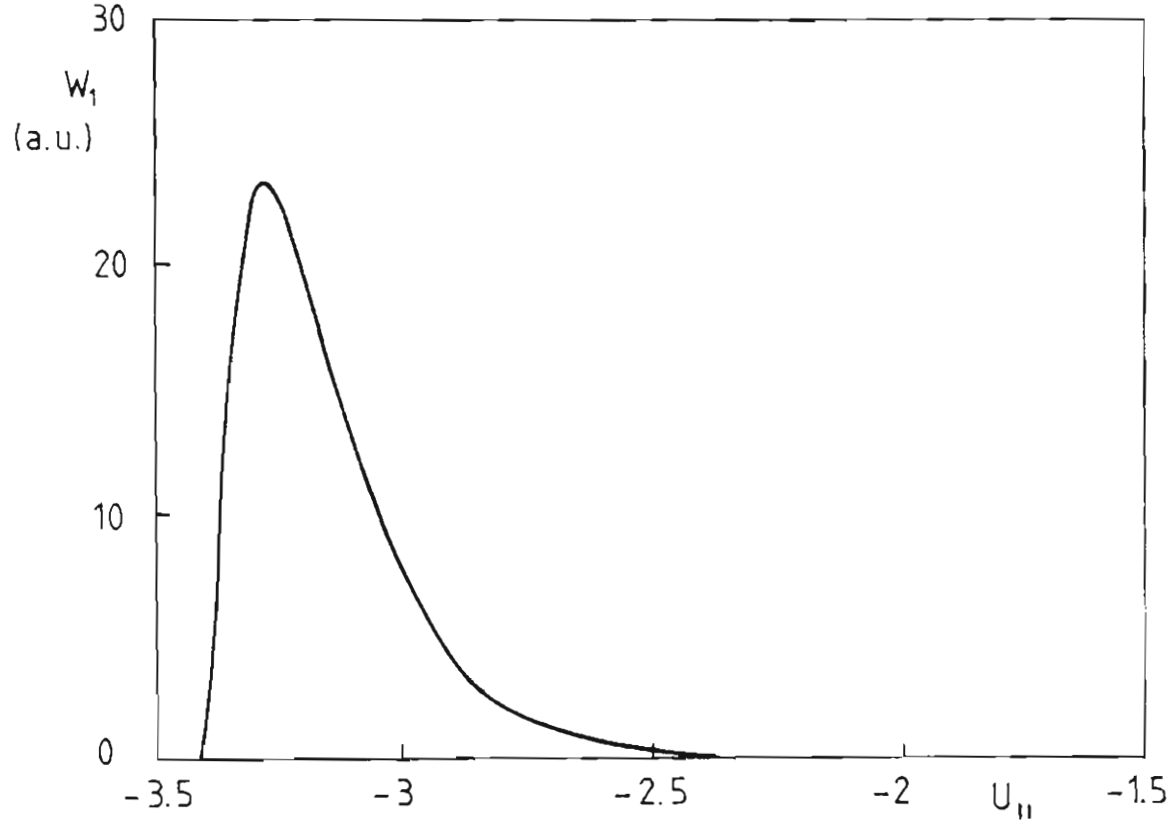

FIG. 2

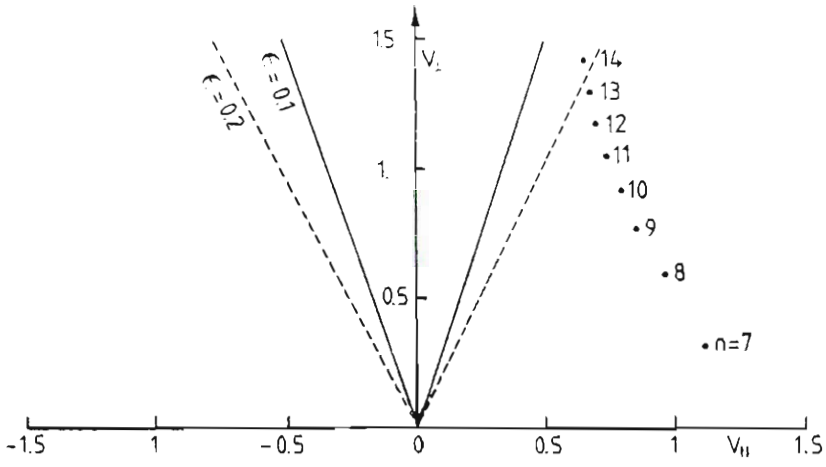

FIG. 3

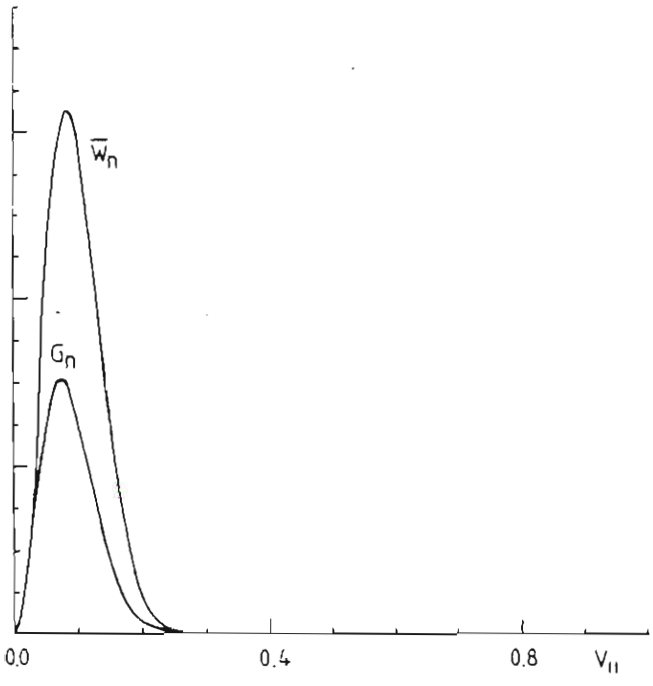

FIG 4

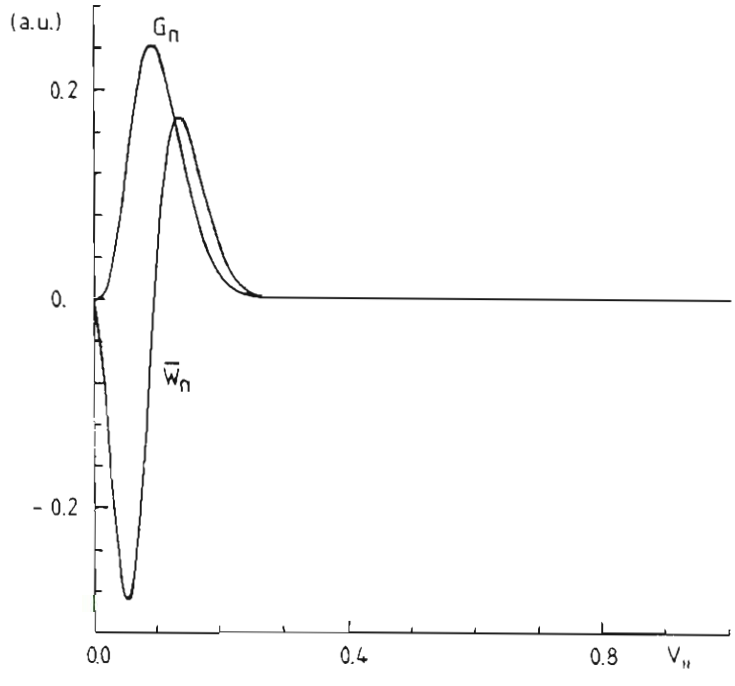

FIG. 5

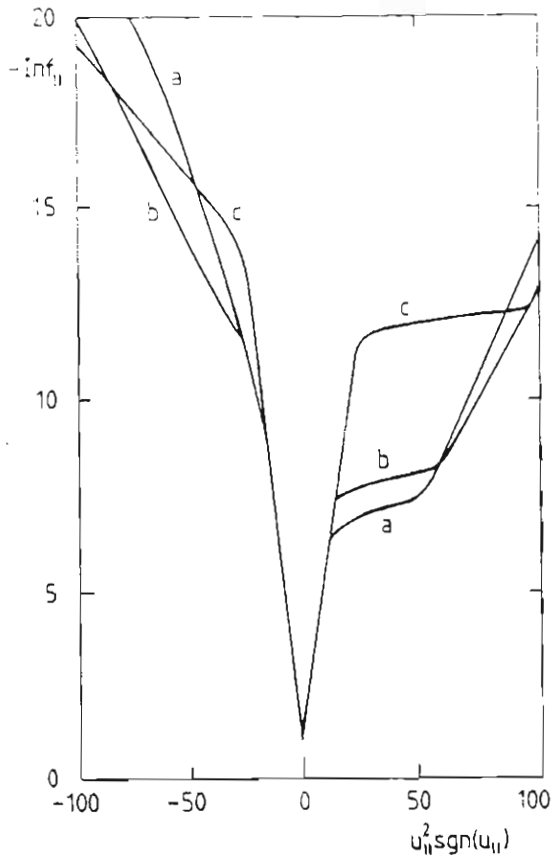

FIG. 6

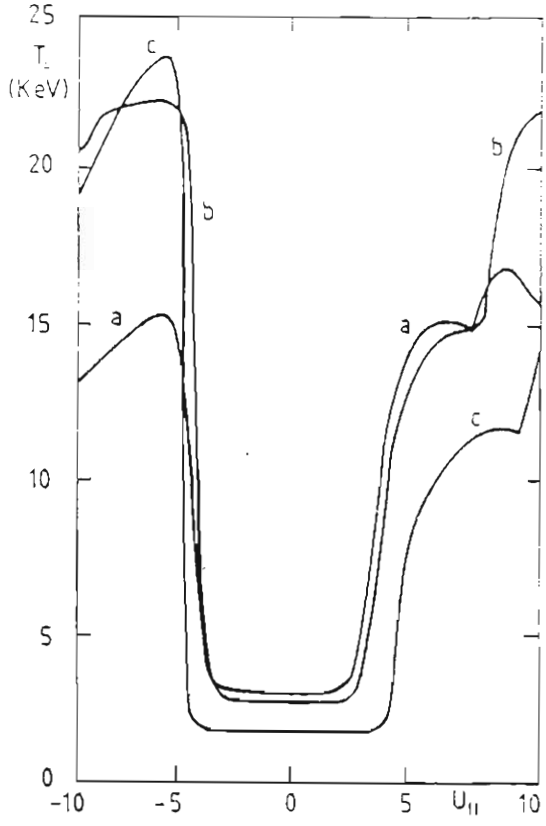

FIG 7

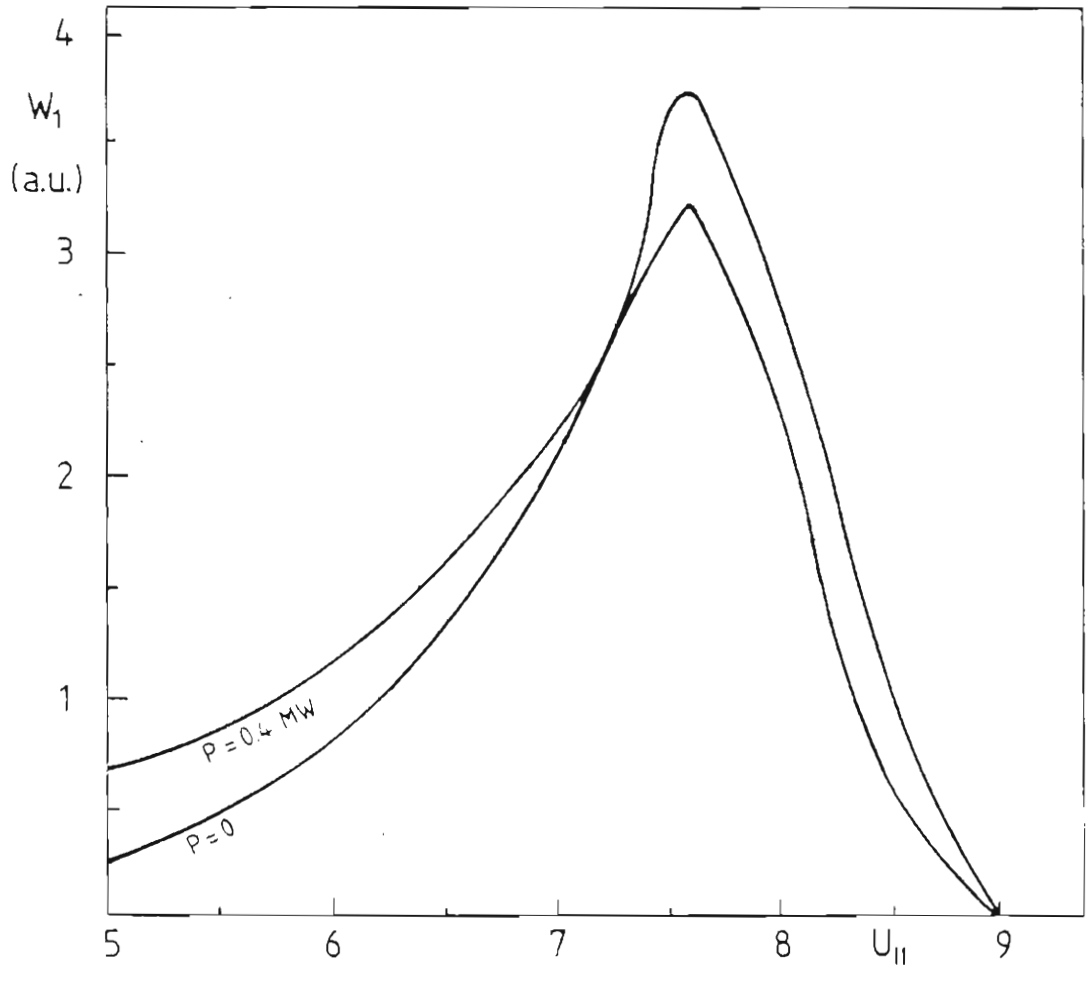

FIG 8

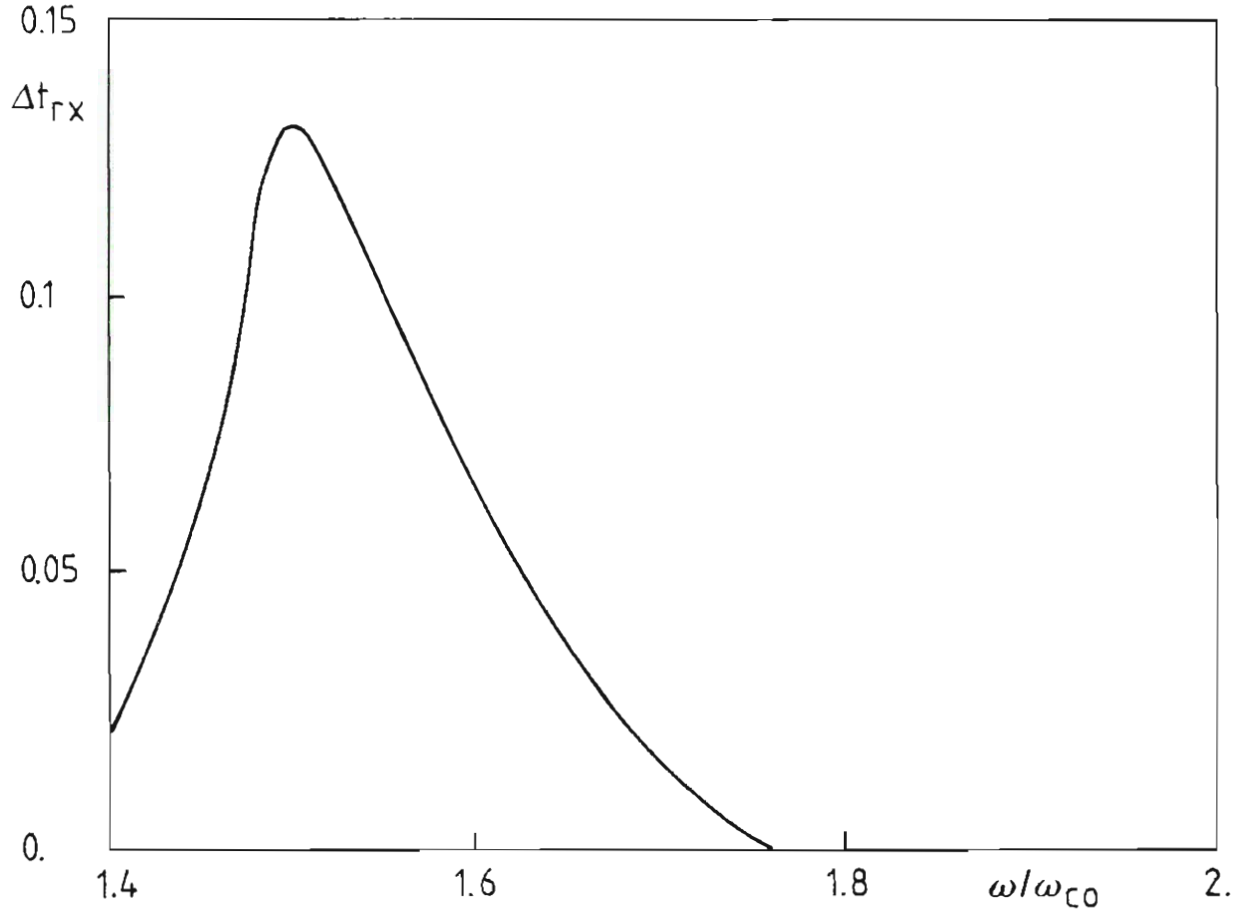
0.15
Δt_{rx}
0.1
0.05
0.
1.4
1.6
1.8
ω/ω_{co}
2.

FIG. 9

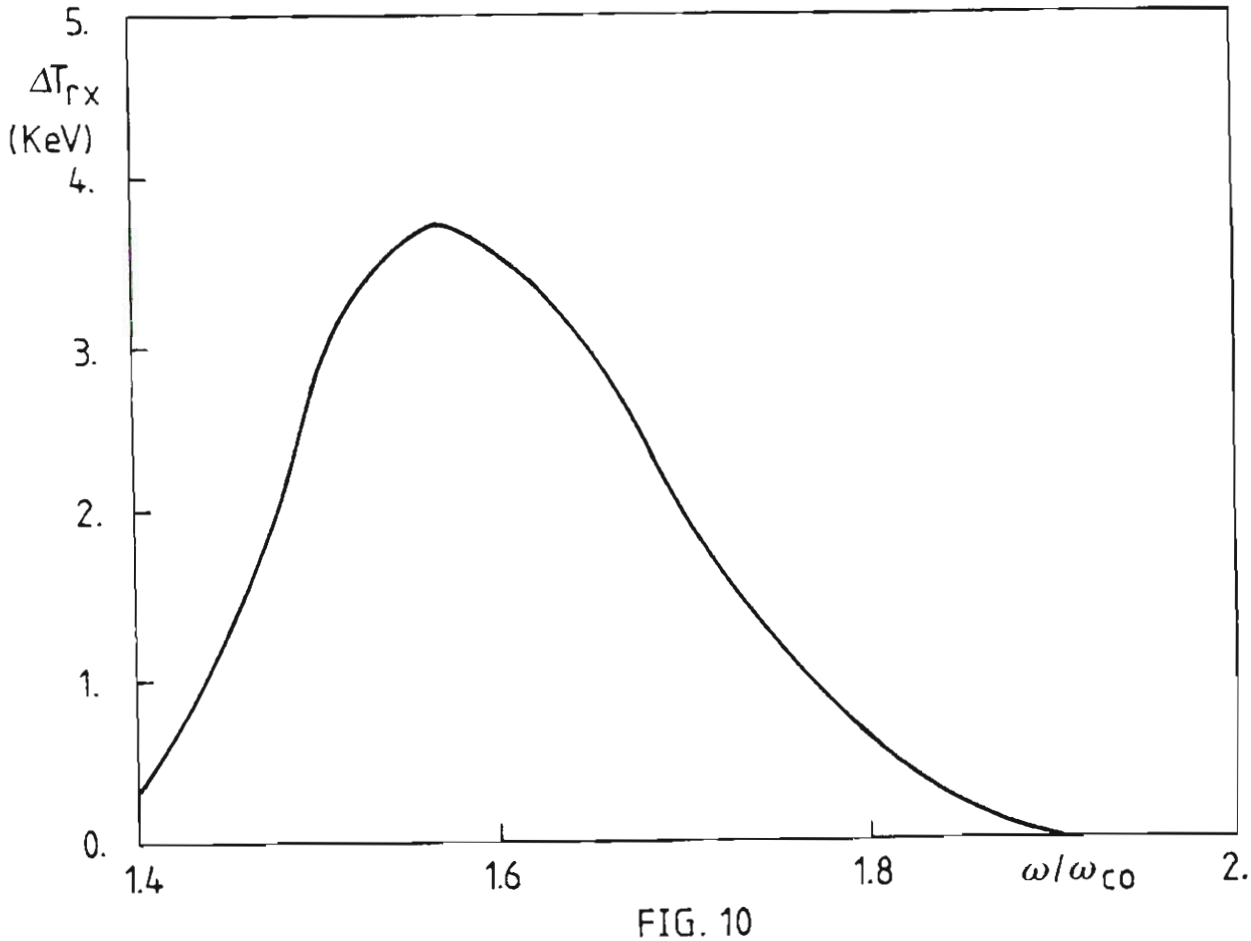
5.
ΔT_{rx}
(KeV)
4.
3.
2.
1.
0.
1.4
1.6
1.8
ω/ω_{co}
2.

FIG. 10